

## Article

# Synthesis, DFT and X-ray Studies of Trans $\text{CuCl}_2\text{L}_2$ with L Is (E)-(4-Chlorophenyl)-N-(3-phenyl-4H-1,2,4-triazol-4-yl)methanimine

Hassan H. Hammud <sup>1,\*</sup>, Moheddine Wehbie <sup>2</sup>, Mohamed M. Abdul-Ghani <sup>3</sup>, Zoltan A. Gal <sup>4</sup>, Malai Haniti Sheikh Abdul Hamid <sup>5</sup> and Nadeem S. Sheikh <sup>5,\*</sup>

<sup>1</sup> Department of Chemistry, College of Science, King Faisal University, P.O. Box 400, Al-Ahsa 31982, Saudi Arabia

<sup>2</sup> Institut de Recherche de Chimie Paris, Chimie Paris Tech-PSL University, 75005 Paris, France

<sup>3</sup> Materia Verte Co., Beirut P.O. Box 11-1919, Lebanon

<sup>4</sup> Oxford Cryosystems, 3 Blenheim Office Park, Long Hanborough, Oxford OX29 8LN, UK

<sup>5</sup> Chemical Sciences, Faculty of Science, Universiti Brunei Darussalam, Jalan Tungku Link, Gadong BE1410, Brunei

\* Correspondence: hhammoud@kfu.edu.sa (H.H.H.); nadeem.sheikh@ubd.edu.bn (N.S.S.)

**Abstract:** A novel approach was carried to prepare trans- $\text{CuCl}_2\text{L}_2$  complex with the ligand L, (E)-(4-chlorophenyl)-N-(3-phenyl-4H-1,2,4-triazol-4-yl)methanimine which was formed in situ during the reaction of  $\text{CuCl}_2$  with 4-(4-chlorobenzylideneamino)-5-phenyl-2H-1,2,4-triazole-3(4H)-thione. The synthesized compounds were characterized by applying various spectroscopic techniques. The crystal structure of the complex was unambiguously determined using X-ray analysis indicating square planar geometry. Intermolecular H-bonds govern the supramolecular structure of the copper complex. Aromatic rings are stacked in an offset packing due to occurrence of  $\pi$ - $\pi$  interactions. The structure is further corroborated with a detailed computational investigation. A thione-thiol tautomerism for the triazole compound was also studied. The Schiff base 1,2,4-triazole copper chloride complex is expected to have high anticancer activity.

**Keywords:** 1,2,4-Triazole; Schiff base; copper complex; DFT studies



**Citation:** Hammud, H.H.; Wehbie, M.; Abdul-Ghani, M.M.; Gal, Z.A.; Sheikh Abdul Hamid, M.H.; Sheikh, N.S. Synthesis, DFT and X-ray Studies of Trans  $\text{CuCl}_2\text{L}_2$  with L Is (E)-(4-Chlorophenyl)-N-(3-phenyl-4H-1,2,4-triazol-4-yl)methanimine.

*Inorganics* **2023**, *11*, 18. <https://doi.org/10.3390/inorganics11010018>

Academic Editors: Saad Shaaban and Wael Mortada

Received: 14 November 2022

Revised: 17 December 2022

Accepted: 22 December 2022

Published: 31 December 2022



**Copyright:** © 2022 by the authors. Licensee MDPI, Basel, Switzerland. This article is an open access article distributed under the terms and conditions of the Creative Commons Attribution (CC BY) license (<https://creativecommons.org/licenses/by/4.0/>).

## 1. Introduction

In the last few decades, the chemistry of 1,2,4-triazole and their fused heterocyclic derivatives have received considerable attention due to their synthetic and effective biological importance. Various 1,2,4-triazole derivatives were found associated with diverse pharmacological activities (Figure 1). The 1,2,4-triazole nuclei were incorporated into a wide variety of therapeutically interesting drug candidates as sedative [1], antifungal [2,3], antiviral [4], insecticidal [5], antimicrobial [6,7], anti-asthmatic [8], anticonvulsants [9], antidepressants [10], plant growth regulator [11], anticancer [12], anti-HIV [13] and anti-inflammatory agents [14]. Moreover, sulfur containing heterocyclic motifs represent an important group of compounds that exhibit a promising practical application [15]. The pharmacological importance of heterocycles derived from 1,2,4-triazole paved the way towards active research in triazole chemistry. As a result, a wide array of novel structures was added to this field every year. In addition, a number of attempts were made to improve the activity of these compounds by varying the substituents on the triazole nucleus [16].

Despite all of the research advances, the resistance towards most of the antibacterial, antifungal and/or antiviral drugs is still a major challenge in medicinal chemistry [17–19]. This issue could be overcome by the preparation of metal complexes, using chelation process via coordination of transition metal ions and development of novel antibiotics [20,21]. Schiff bases inherently possess a strong ability to form metal complexes [22] with interesting biological properties [23–26]. The Co(II), Ni(II), Cu(II) and Zn(II) complexes of Schiff

bases are biologically relevant and they exhibit enhanced bioactivities compared to their parent ligands. Owing to substantial biological activities associated with the triazole derivatives [27–29] both Schiff bases containing a triazole moiety, as well as their metal complexes are expected to exhibit promising levels of bioactivities. At the same time, the process of chelation causes radical changes in the biological properties of the ligands and of the metal motif. It was reported that chelation improves the treatment of many diseases including cancer. In addition, a number of Schiff base complexes [22,30,31] were tested for their antibacterial [32,33], antifungal [34], anticancer [35,36] and herbicidal activities [37].

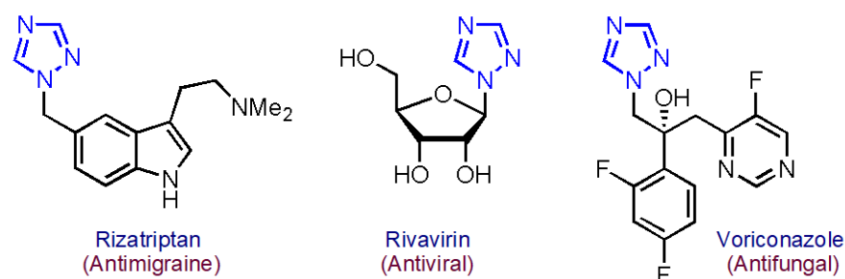


**Figure 1.** Representative bioactive molecules containing 1,2,4-triazole structural motif.

Herein, we report on an efficient approach to preparing the copper complex  $\text{trans-CuCl}_2\text{L}_2$ . The ligand L, (E)-(4-chlorophenyl)-N-(3-phenyl-4H-1,2,4-triazol-4-yl)methanimine, was synthesized in situ by the reaction of copper chloride with 4-(4-chlorobenzylideneamino)-5-phenyl-2H-1,2,4-triazole-3(4H)-thione during the preparation of the complex. All the synthesized compounds were characterized by applying various spectroscopic techniques. The complex was characterized by infrared and UV–visible spectroscopy and its crystal structure was determined using X-ray analysis which is further corroborated with a detailed computational investigation.

## 2. Results and Discussion

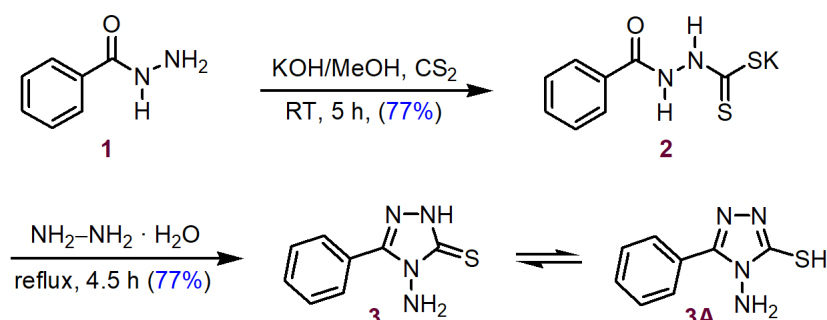
The acid hydrazide, namely benzhydrazide (1), was chosen to prepare the desired ligand which was initially reacted with carbon disulfide under basic conditions to prepare the dithiocarbazinate (2). Later, this was cyclized with hydrazine under reflux conditions to afford the required 4-amino-5-phenyl-3-mercapto-(4H)-1,2,4-triazole (3) followed by condensation with a chlorobenzaldehyde (4) to yield the corresponding Schiff base 5. Finally, the obtained Schiff base was treated with copper chloride to synthesize the desired crystalline Schiff base complex (6). A detailed account of the synthesis and characterization is provided below.

### 2.1. Synthesis of 4-amino-5-aryl-3-mercapto-(4H)-1,2,4-triazole (3)

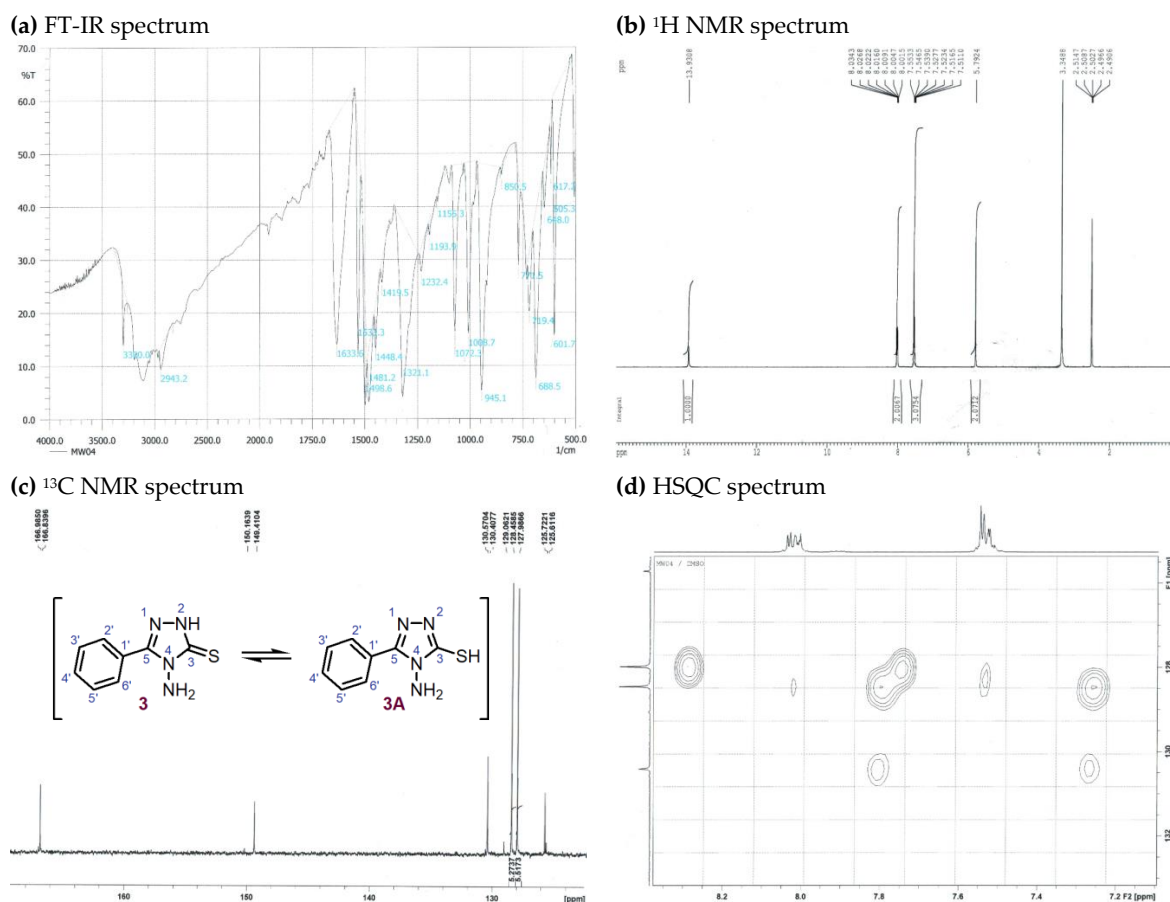
Commercially available benzhydrazide (1) was treated with carbon disulfide in alcoholic potassium hydroxide solution to provide potassium dithiocarbazinate (2), and then refluxed with an excess of hydrazine hydrate (Scheme 1). During the course of the reaction, both discoloration of the reaction mixture and evolution of hydrogen sulfide gas were observed. Upon completion of the reaction, the mixture was cooled and quenched under acidic conditions. This led to the formation of white precipitate of 4-amino-5-aryl-3-mercapto-(4H)-1,2,4-triazole (3A) in excellent yield which is known to exist in equilibrium with its thione tautomer (3) [38]. The triazole derivative (3) was fully characterized by spectroscopic techniques including IR,  $^1\text{H}$  NMR,  $^{13}\text{C}$  NMR, COSY and HSQC to confirm its structure.

The IR spectrum for the compound (3) is consistent with the given structure (Figure 2a). The spectra for the triazole (3) shows the presence of two absorptions for the primary  $\text{NH}_2$  group at  $3300\text{--}3180\text{ cm}^{-1}$  and a single absorption for the triazole N–H at  $3100\text{ cm}^{-1}$ . A peak for the C=N group appears at the expected region  $1633\text{ cm}^{-1}$  while the C=S group appears at  $1321\text{ cm}^{-1}$ . In addition to these characteristic peaks for triazole (3), the expected absorption peaks for the aromatic ring were also noted. The  $^1\text{H}$  NMR spectrum ( $\text{DMSO-}d_6$ )

for the triazole (**3**) proved its structure. The assignments are based on  $^1\text{H}$  NMR (Figure 2b) and 2D-HSQC NMR spectra (Figure 2d), in addition to the reported literature data [39,40]. The absorption observed downfield at 13.93 ppm is cautiously assigned to the S–H bond or to the N–H of the triazole ring. This is debatable due to the fact that some of the literature reports indicate such absorptions for “S–H” [28,41], while some reports describe them for the corresponding “N–H” bond [32,42]. In addition, there are literature precedents where these absorptions are documented for “N–H or S–H” [13,43]. The peak for free  $\text{NH}_2$  is clearly observed at 5.7–5.8 ppm, in addition to the peaks for the hydrogen atoms of the phenyl ring at 8.02 (m, 2H, 2' and 6'), 7.53 (m, 3H, 3', 4' and 5'). The  $^{13}\text{C}$ -NMR spectrum for the compound **3** clearly suggests the formation of expected triazole structure (Figure 2c). The spectrum shows six carbon signals including the C-3 and C-5 of the triazole ring at 166.83 ppm and 149.41 ppm, respectively. The peaks for the carbon atoms of the phenyl ring are observed at 130.4 ppm (C-4'), 128.45 ppm (C-3' and C-5'), 127.98 ppm (C-2' and C-6') and 125.72 ppm (C-1').



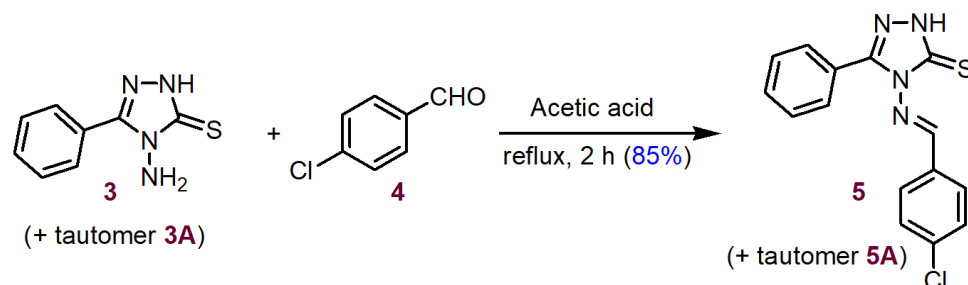
**Scheme 1.** A two-step synthesis of 1,2,4-triazole derivative and its thione–thiol tautomerism (**3**) and (**3A**).



## 2.2. Preparation of the Schiff base

### 4-(4-chlorobenzylideneamino)-5-phenyl-2H-1,2,4-triazole-3(4H)-thione (5)

The desired Schiff base (5) was prepared in acetic acid (mild acidic conditions) by the treatment of 4-amino-3-mercapto-5-phenyl-(4H)-1,2,4-triazole (3) with commercially available chlorobenzaldehyde (4) (Scheme 2). The obtained yellow crystalline product (5) was fully characterized by IR,  $^1\text{H-NMR}$  and  $^{13}\text{C-NMR}$  which confirms its structure.



**Scheme 2.** Synthesis of Schiff base 5.

The IR spectra for compound (5) confirms the formation of the Schiff base (Figure 3a). The disappearance of the  $\text{NH}_2$  absorptions and the presence of a new absorption at about  $1607\text{ cm}^{-1}$  is assigned for the characteristic  $\text{CH}=\text{N}$  of the Schiff base. This indicates that the condensation reaction between the triazole amino group and the aromatic aldehyde proceeded smoothly. The IR spectra also shows the expected  $\text{N-H}$  absorption peak at  $3111\text{ cm}^{-1}$ , meanwhile, the  $\text{S-H}$  absorption peak is observed at  $2750\text{ cm}^{-1}$ . The vibration related to  $\text{C}=\text{S}$  is noticed at  $1279\text{ cm}^{-1}$ , while the  $\text{N-C-S}$  appeared at  $960\text{ cm}^{-1}$ , in addition to the expected out of the plane absorptions of the aromatic rings at  $880\text{ cm}^{-1}$ . The assignment of  $\text{N-H}$ ,  $\text{S-H}$ ,  $\text{CH}=\text{N}$ ,  $\text{C}=\text{S}$  and  $\text{N-C-S}$  bands are based on the literature data. The  $^1\text{H-NMR}$  spectra ( $\text{DMSO-}d_6$ ) for compound (5) is in accordance with the formation of the Schiff base (Figure 3b). The observed singlet at 5.7 ppm for the amino  $-\text{NH}_2$  protons of the starting aminotriazole (3) was replaced by a new peak in the range 9.76 ppm assigned to the  $\text{CH}=\text{N}$  proton. This is a clear indication of the successful condensation reaction leading to the Schiff base (5). The  $^1\text{H-NMR}$  spectrum also reflects the presence of the phenyl ring attached to C-5 of the triazole ring, in addition to the chlorophenyl group. The “ $\text{S-H/N-H}$ ” triazolic proton is shown downfield in the region at 14.1 ppm. The  $^1\text{H-NMR}$  spectra for the Schiff base (5) provides two sets of multiplets for the phenyl substituent. The first ranging at 7.88 ppm with 2H integration is assigned to protons at positions 2' and 6', while the second multiplet at 7.53 ppm with 3H integration is assigned to protons at positions 3', 4' and 5'. The protons located at positions 2' and 6' are present at lower field due to the anisotropic field effect of the 1,2,4-triazole ring. In addition, the chlorophenyl aromatic protons of the Schiff base (5) are also in agreement with the given structure. It shows two doublets for a typical *para*-substituted benzene ring; one doublet is due to protons present at positions 2'' and 6'', while the second doublet is for the protons located at the positions 3'' and 5'', which reflects a typical  $\text{AA}'\text{BB}'$  system. Thus, the peaks at 7.9 (d,  $J = 8.5$ , 2H, 2'' and 6'') and 7.65 (d,  $J = 8.5$ , 2H, 3'' and 5'') are attributed to the chlorobenzyl ring.

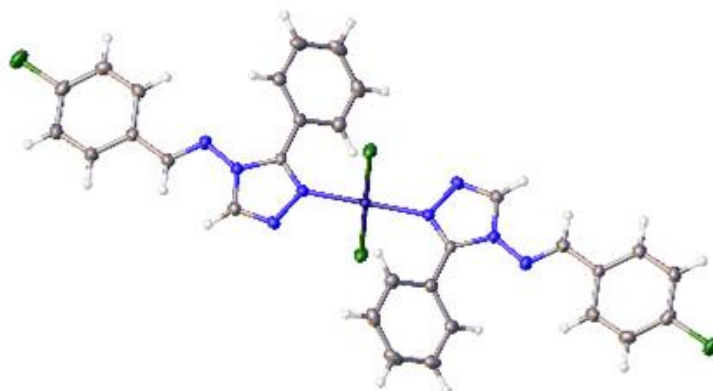


section, the filtration technique was used in order to remove the side product green precipitate before crystallization of the desired copper complex. The violet filtrate was left for slow evaporation and violet pure crystals were then obtained. Obtaining the product in a crystalline form is considered as a way of purifying the product, because it is well known that the crystalline product should have a much higher purity compared to the amorphous product. Also, the morphology of the crystals was checked using a microscope. The crystals appeared as perfect crystalline transparent violet cubes of high purity with no amorphous materials adsorbed on them. Finally, elemental analysis is particularly important to determine the purity of the sample. The theoretical% elemental analysis for complex (6)  $C_{30}H_{22}Cl_4CuN_8$  (699.88 g/mol) is: %C, 51.48%; %H, 3.17%; %Cl, 20.26%; %Cu, 9.08%; %N, 16.01%. Meanwhile, the X-ray single structure CIF file is in CCDC No. 2217976 which contains the supplementary crystallographic data for complex (6), Table S1 (Supplementary Materials).

The crystal structure demonstrated that the crystal system is monoclinic with a space group  $P2_1/c$ . Copper in complex (6) adopts a square planar coordination (Cu(1A)Cl(2A)N(1AA)Cl(2A<sup>1</sup>)N(1AA<sup>1</sup>) (Figure 4a). Thus, N(1AA) of triazole of one ligand L, and N(1AA<sup>1</sup>) of a second triazole of another ligand L are *trans* to each other. The coordinated nitrogen atoms are perfectly linear with central copper(II) ion. The angle N(1AA)Cu(1A)N(1AA<sup>1</sup>) is equal to 180 (°). Additionally, the angle Cl(2A)Cu(1A)Cl(2A<sup>1</sup>) is equal to 180.0 (°). The other angles involved are orthogonal with little deviations: Cl(2A)Cu(1A)N(1AA) and Cl(2A<sup>1</sup>)Cu(1A)N(1AA<sup>1</sup>) are 91.36 (5) (°) and 91.37 (5) (°). Meanwhile, the angles Cl(2A<sup>1</sup>)Cu(1A)N(1AA) and Cl(2A)Cu(1A)N(1AA<sup>1</sup>) are equal to 88.64 (5) (°) and 88.63 (5) (°), respectively. Each distance of the bonds Cu1A–Cl2A and Cu1A–Cl2A1 is equal to 2.2552 (7) Å. Meanwhile, the bond distance between Cu(1A) and each of N(1AA) or N(1AA<sup>1</sup>) is equal to 1.9603 (18) Å. The triazole ring and phenyl ring are not coplanar; they form an angle of 37.75 (°). This deviation could be due to the steric effect.

Intermolecular H-bonds govern the supramolecular structure of the copper complex (6). Both chloride ions and nitrogen N(4) atoms of triazoles are involved in hydrogen bonds with CH groups (Figure 4b). For the D–H...A H-bond systems, C(0AA)–H(0A) ... Cl(2A) and C(12)–H(12) ... Cl(2A), the distances  $d(D...A)$  are 3.549 and 3.735 (Å) and the angles (DHA) are 167.99 and 163.61 (°), respectively. While for the H-bonds C(18)–H(18) ... N(4), the distance is 3.333 (Å) and the angle is 150.63 (°). The  $\pi$ – $\pi$  interactions between aromatic rings occur when the rings are stacked in an offset or slipped packing [44]. The aromatic rings are parallel displaced. The  $\pi$ – $\pi$  interactions are dipole–dipole electrostatic interactions between the different permanent and static molecular charge distributions caused by substituents on the ring. These van der Waal interactions are attractive and their potentials fall off rapidly with distance  $1/r^6$ . In addition,  $\pi$ – $\sigma$  attractions can dominate between the  $\pi$ -electrons of the rings and the positively charged hydrogen atoms [44,45]. These attractive forces overcome the  $\pi$ – $\pi$  Pauli repulsions in an offset  $\pi$ -stacked geometry according to the Hunter–Sanders rules. Pauli repulsion is caused by the filled electron clouds of interacting molecules that overlap at short distances [44–48]. The order of stability in the interaction of two  $\pi$  systems is  $\pi$ -deficient– $\pi$ -deficient >  $\pi$ -deficient– $\pi$ -rich >  $\pi$ -rich– $\pi$ -rich [44–49]. The aromatic rings arrangement in the complex (6) between  $\pi$ -rich triazole of one copper complex and  $\pi$ -deficient chlorophenyl of a neighboring copper complex is a  $\pi$ – $\pi$  stacked in an offset packing (slipping). The interplanar angle between the aryl rings is 13.43 (°). The atoms contacts in Å are N(1AA)–C(20) (3.652); N(4)–C(21) (3.625); C(5)–C(18) (3.787); N–C(15) (3.535) and C(0AA)–C17(3.394). The centroid–centroid (triazole C(5)NC(0AA)N(4)N(1AA)–phenyl chloride C(20)C(21)C(19)C(17)C(15)C(18) separation between the two slipped rings is 3.562 Å. Thus, the separation of 3.562 Å of the rings in complex (6) is the result of strong  $\pi$ – $\pi$  interactions.

(a) Asymmetric unit of square planar trans-CuCl<sub>2</sub>L<sub>2</sub> (**6**)  
 [L = (E)-(4-chlorophenyl)-N-(3-phenyl-4H-1,2,4-triazol-4-yl)methanimine]



(b)  $\pi$ - $\pi$  Interactions in CuCl<sub>2</sub>L<sub>2</sub> (**6**).  
 (Atoms contacts and centroid-centroid separations)

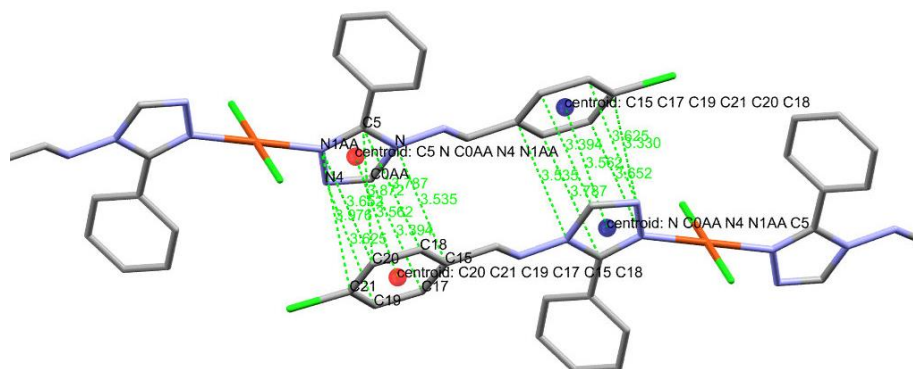


**Figure 4.** X-ray structure and structural features for square planar trans-CuCl<sub>2</sub>L<sub>2</sub> **6**.

Additionally, the UV-visible spectra is shown in Figure S1. The peak at  $\lambda_{\text{max}}$  307 nm is mainly due to d-d transition with shoulders at 277, 287 and 302 nm.

The FTIR spectra of CuCl<sub>2</sub>L<sub>2</sub> complex (**6**) is depicted in Figure 5. The main peak that appeared at 3092.1 cm<sup>-1</sup> is due to aromatic C-H stretch. Meanwhile, imine >C=N and aromatic >C=C< stretches occurred at 1596.3 cm<sup>-1</sup>.

Regarding the loss of the sulfur atom during the complexation with CuCl<sub>2</sub>, we are still investigating this experimental observation to fully understand the mechanism involved. One of the plausible explanations could be related to the complexation with copper chloride that could facilitate this rearrangement as reported for other systems, where copper chloride was involved in the rearrangement of an ampicillin-containing sulfur moiety [49]. Sulfur was likely lost in the form of H<sub>2</sub>S gas due to compound (**5**) rearrangement, while using NaOH then HCl to neutralize the medium, assisted by copper complexation as observed in other similar system [49]. The detailed mechanism is still under investigation. Thus, the obtained ligand L: (E)-(4-chlorophenyl)-N-(3-phenyl-4H-1,2,4-triazol-4-yl)methanimine was formed in situ by the reaction of CuCl<sub>2</sub> with 4-(4-chlorobenzylideneamino)-5-phenyl-2H-1,2,4-triazole-3(4H)-thione (**5**) followed by the formation of the complex CuCl<sub>2</sub>L<sub>2</sub> (**6**).

It is also expected that the Schiff base complex trans-CuCl<sub>2</sub>L<sub>2</sub> (**6**) should show better anticancer activity than its ligand, based on the cytotoxicity studies for related copper complexes [48–51]. Thus, the study of the anticancer behavior of the copper complex (**6**) will be carried out in a future work.

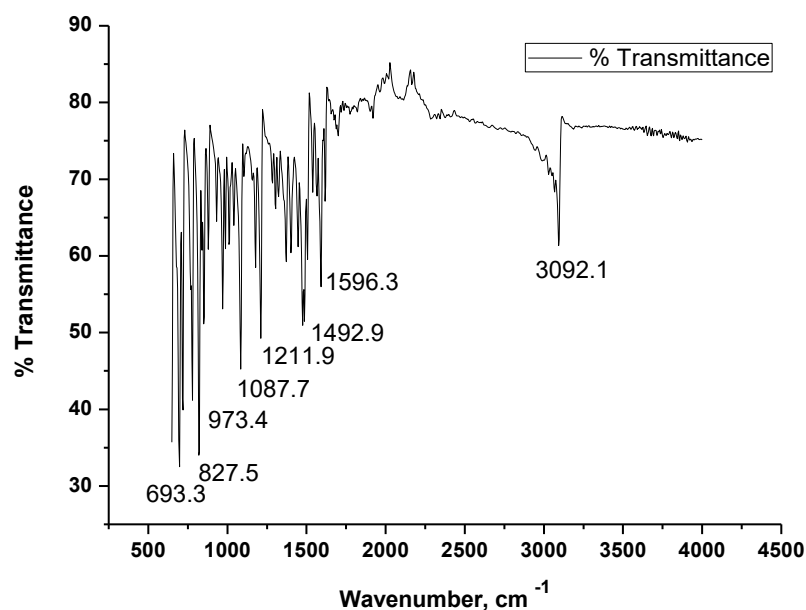


Figure 5. FTIR spectrum of the copper complex (6).

#### 2.4. Computational Investigation

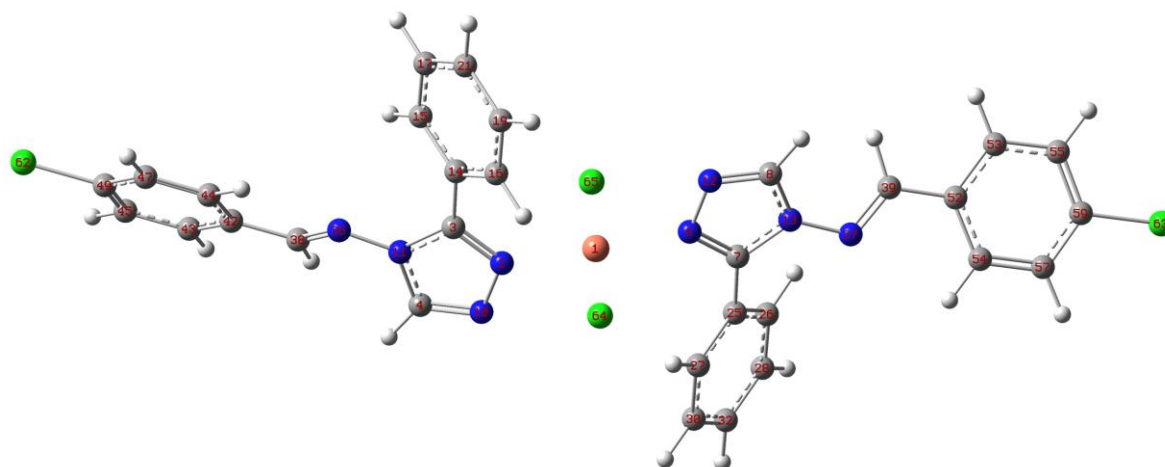
A detailed computational investigation was carried out to corroborate the experimental X-ray data for the Cu<sup>(II)</sup> complex (Table S2). Initial screening was conducted by applying different hybrid and pure functionals implemented in the Gaussian package using 6-31G(d) basis set. The results are delineated in Table 1 and to our delight, all the methods furnished an excellent linear relationship (Figure S2) between the experimental and computed values for the bond lengths of the atoms which are pivotal to impart the structural features. These atoms are in close proximity to the Cu atom, belong to 1,2,4-triazole ring, the carbon atoms which are connected with the triazole ring and also the C–Cl bond present in benzylidene motif.

Table 1. Comparison of selected experimental and calculated bond lengths (Å) for the Cu<sup>(II)</sup>-complex (6) using 6-31G(d)/LanL2DZ mixed basis set.

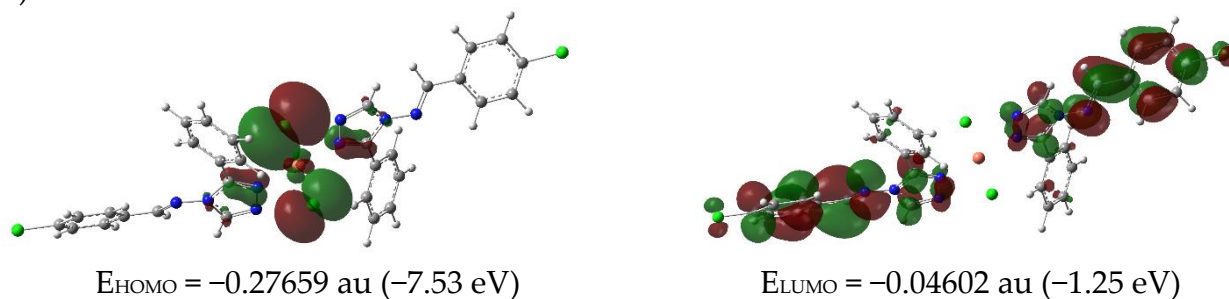
	Atoms *	Experimental	CAM-B3LYP	$\omega$ B97XD	B3LYP	MPW1PW91	B3PW91	PBEPBE
1	Cu1–Cl65	2.2552	2.32245	2.32583	2.35151	2.32697	2.33641	2.36238
2	Cu1–N6	1.9603	1.98980	1.99478	2.01025	1.99702	1.99994	1.99434
3	N6–N12	1.3780	1.36072	1.35936	1.36874	1.35584	1.35925	1.37069
4	N6–C7	1.3010	1.31391	1.31499	1.32261	1.31716	1.32039	1.33439
5	N12–C8	1.2890	1.29647	1.29993	1.30322	1.29924	1.30190	1.31503
6	N13–C8	1.3610	1.37361	1.37337	1.38006	1.37290	1.37556	1.38594
7	N13–C7	1.3600	1.36775	1.36506	1.37806	1.36936	1.37323	1.38636
8	C7–C25	1.4540	1.46381	1.46333	1.46439	1.45853	1.46011	1.46150
9	N13–N37	1.3840	1.37593	1.37701	1.37927	1.36791	1.37086	1.37838
10	N37–C39	1.2670	1.27635	1.27852	1.28583	1.28112	1.28432	1.29893
11	C39–C52	1.4490	1.46268	1.46373	1.46148	1.45706	1.45818	1.45929
12	Cl63–C59	1.7300	1.77717	1.77651	1.79155	1.77405	1.77941	1.79058

\* The numbers described here for the atoms are according to the numbers mentioned for the optimized geometry of the complex in Figure 6a, generated during the visualization using GaussView software.

## (a) Optimized geometry



## (b) Frontier molecular orbitals



## (c) ESP map

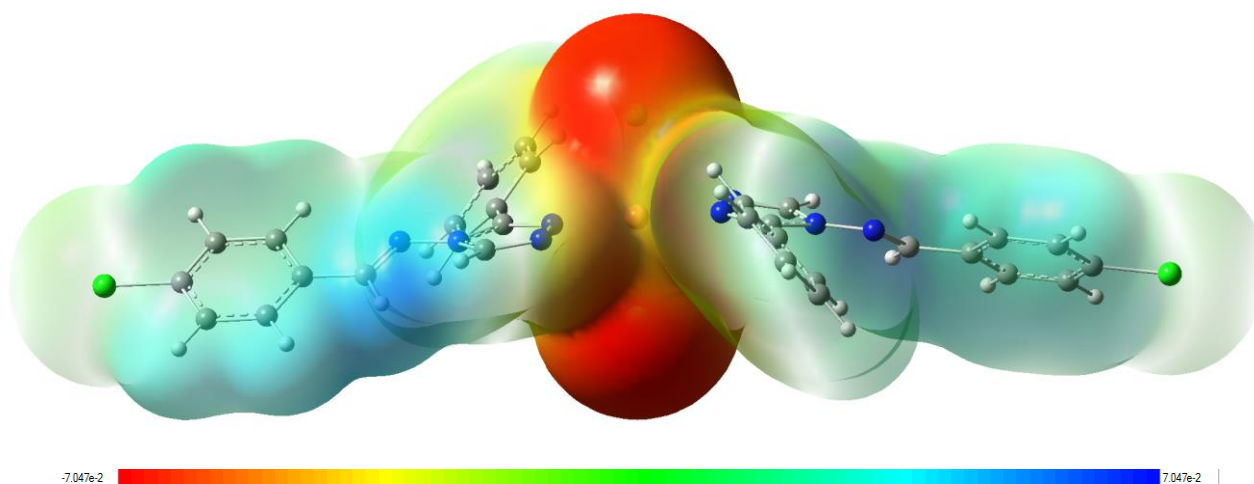


**Figure 6.** Optimized structure (a), frontier molecular orbitals (b) and electrostatic potential map (c) for the Cu<sup>(III)</sup>-complex (6) calculated at CAM-B3LYP/6-31G(d)/LanL2DZ level of theory.

A judicious comparative analysis for the data revealed that the CAM-B3LYP method is the most appropriate to simulate the Cu–Cl, Cu–N and other bonds present in the triazole ring. More or less a similar observation was noticed for the  $\omega$ B97XD method. All other functionals applied in this study, and as mentioned in Table 1, provided variable levels of correlation compared with the experimental values.

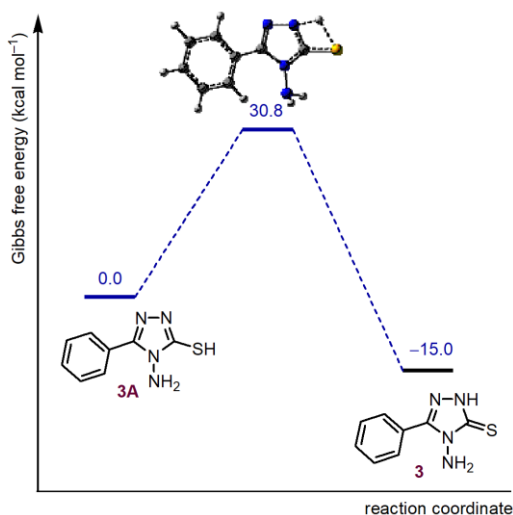
With the comparative data in hand and in order to evaluate the effect of different basis sets, further calculations were performed using CAM-B3LYP method (Table S3). As expected, a strong correlation was observed for other basis sets as well (Figure S3), however

the addition of diffuse function offered a slightly poor agreement between the computed and experimental bond length values when compared with the basic 6-31G(d)/LanL2DZ basis set. This is in agreement with our previous findings for the zinc<sup>(II)</sup> hydroxyethyladenine complex [52].

The optimized structure of the Cu<sup>(II)</sup>-complex (6) is presented in Figure 6a. An analysis of the frontier molecular orbitals reveals that HOMO is located on the Cu and atoms which are directly linked with it, however LUMO is extended over the triazole ring and benzylidene moiety (Figure 6b). Moreover, the electrostatic potential map illustrates the presence of lowest potential on Cl atoms linked with the Cu atom, representing this part of the complex as the most electron rich site (Figure 6c).

In order to study the thione–thiol tautomerism for the triazole (3) and (3A), computational calculations were applied which suggested that the thione form (3) is 15 Kcal mol<sup>−1</sup> more stable compared to its corresponding thiol structure (3A) (Figure 7a; Table S4). It also required a higher activation barrier (30.8 Kcal mol<sup>−1</sup>) for this conversion. Computed bond dissociation enthalpies (BDEs) for thione–thiol tautomers also provided further evidence supporting the increased stability of the thione tautomer (3) (Figure 7b). The BDE for the S–H bond in thiol (3A) is 15.4 Kcal mol<sup>−1</sup> less than the BDE for the N–H bond in thione (3). This leads to the facile cleavage of the S–H bond of thiol (3A), leading to its conversion into the more stable thione tautomer (3).

(a)  $E_a$  and  $E_R$  for thione–thiol tautomerism



(b) BDE for N–H and S–H bonds

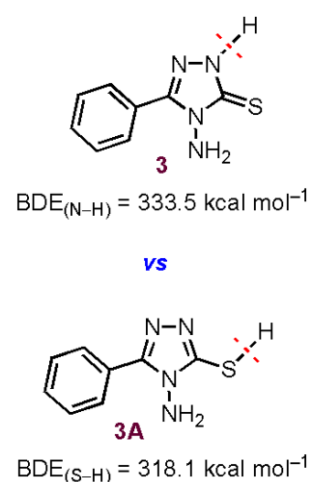


**Figure 7.** Energy of activation ( $E_a$ ) and reaction energy ( $E_R$ ) for the thione–thiol tautomers (3) and (3A) (a) and bond dissociation energies (BDE) for N–H and S–H bonds in thione 3 and thiol 3A structures, respectively, (b), computed at B3LYP/6-31+G(d,p) level of theory.

### 3. Experimental

#### 3.1. X-ray Crystallography

Single crystals of the copper complex were mounted in inert oil and transferred to the diffractometer with cold gas stream. The crystal data and structure of copper complex was then determined, Table S1. The obtained formula was C<sub>30</sub>H<sub>22</sub>N<sub>8</sub>Cl<sub>4</sub>Cu and the molar mass  $M = 699.90$  g/mol, monoclinic. The Crystal Data also indicated  $a = 10.933(2)$  Å,  $b = 13.1221(14)$  Å,  $c = 11.2068(16)$  Å,  $\beta = 114.68(2)^\circ$ ,  $U = 1460.9(4)$  Å<sup>3</sup>,  $T = 150.0$ , space group P21/c (no. 14),  $Z = 2$ ,  $\mu(\text{Mo K}\alpha) = 1.151$ . A total of 10555 reflections were measured and 2661 unique ( $R_{\text{int}} = 0.0375$ ) were used in all calculations. The final  $wR(F2)$  was 0.0779 (all data). The report was created by Olex2.

#### 3.2. Computational Method

Density functional theory (DFT) [53] calculations were performed using Gaussian 09 (revision E.01) [54] and the Gaussview [55] was used to generate input geometries and visu-

alize output structures. Regarding geometry optimizations and frequency calculations for the Cu(II) complex, different functionals (B3LYP [56–58], CAM-B3LYP [59], B3PW91 [57,60], MPW1PW91 [61],  $\omega$ B97XD [62], and PBEPBE [63]) implemented in the Gaussian program were used with the 6–31G(d) basis set for C, H and N atoms [52], while the LanL2DZ [64–66] basis set was used to describe the Cu and Cl atoms. To obtain further insight, higher basis sets were also used with the most appropriate method. All stationary points were characterized as minima and thermal corrections were computed from unscaled frequencies, assuming a standard state of 298.15 K and 1 atm.

### 3.3. Synthesis of Potassium Benzdithiocarbazine (2)

Potassium benzdithiocarbazine (2) was prepared from benzoic acid hydrazide (1) by treatment with carbon disulfide and potassium hydroxide in methanol as reported in the literature [67]. The spectroscopic data were in complete agreement with the literature.

### 3.4. Synthesis of 4-amino-3-mercapto-5-phenyl-(4H)-1,2,4-triazole (3)

The obtained benzdithiocarbazine (2, 17 g, 68 mmol) was refluxed for 4.5 h with hydrazine hydrate (34 g, 680 mmol) to prepare 4-amino-3-mercapto-5-phenyl-(4H)-1,2,4-triazoles (3) [68–70] which was obtained as white crystals (10 g, 52.2 mmol, 77%); m.p. = 198–200 °C. FT-IR (KBr)  $\nu$  = 3300 and 3180 (NH<sub>2</sub>), 3100 (N–H) 2756 (S–H), 1633 (C=N), 1232 (C=S) cm<sup>−1</sup>. <sup>1</sup>H-NMR (DMSO-*d*<sub>6</sub>)  $\delta$  = 13.93 (s, 1H, S–H or N–H), 8.03–8 (m, *J* = 2.25, 2H, Ar-H-2,6), 7.55–7.51 (m, *J* = 2.04, 3H, Ar-H-3,4,5), 5.7 (s, 2H, NH<sub>2</sub>) ppm. <sup>13</sup>C-NMR (DMSO-*d*<sub>6</sub>)  $\delta$  = 166.83, 149.41, 130.4, 128.45, 127.98, 125.72.

### 3.5. Synthesis of 4-(4-chlorobenzylideneamino)-5-phenyl-2H-1,2,4-triazole-3(4H)-thione (5)

A mixture of 4-amino-5-phenyl-3-mercapto-4H-1,2,4-triazole (3, 0.5 g, 2.6 mmol) and chlorobenzaldehyde (4, 0.37 g, 2.6 mmol) in acetic acid (10 mL) was heated under reflux for 2 h. After cooling the obtained solid precipitate was filtered, washed with cold acetic acid, then with hot water and crystallized from ethanol affording 4-(4-chlorobenzylidene) amino-3-mercapto-5-phenyl-4H-1,2,4-triazole (5) [68–70], which was obtained as yellow crystals (0.7 g, 2.2 mmol, 85%); m.p. = 212–213 °C. FT-IR (KBr)  $\nu$  = 3111 (N–H), 2750 (S–H), 1607 (C=N), 1279 (C=S), 960 (N–C–S) cm<sup>−1</sup>. <sup>1</sup>H-NMR (DMSO-*d*<sub>6</sub>)  $\delta$  = 14.1 (bs, 1H, S–H or N–H), 9.76 (s, 1H, CH=N), 7.9 (dd, *J* = 8.5, 4.9 Hz, 2H, Cl–Ph–H-2,6), 7.88 (m, 2H, Ph–H-2,6), 7.65 (dd, *J* = 8.5, 4.9 Hz, 2H, Cl–Ph–H-3,5), 7.53 (m, 3H, Ph–H-3,4,5) ppm. <sup>13</sup>C-NMR (DMSO-*d*<sub>6</sub>)  $\delta$  = 165.7, 162.7, 148.99, 137.89, 131, 130.7, 129.79, 129.09, 128.6, 125.7, 121.56) ppm.

### 3.6. Preparation of Trans-Copper Dichloride bis(E)-(4-chlorophenyl)-N-(3-phenyl-4H-1,2,4-triazol-4-yl)methanimine, CuL<sub>2</sub>Cl<sub>2</sub> (6)

A solution of copper (II) chloride (0.175 g, 1 mmol) in ethanol (10 mL) and a solution of sodium hydroxide (0.04 g, 1 mmol) in ethanol (10 mL) was added to 10 mL of hot ethanolic solution of the Schiff base (5, 0.314 g, 1 mmol) and then neutralized by adding dil. HCl. The resultant solution was boiled for about two hours and a green powder was formed (probably copper hydroxide side-product). The green precipitate was separated by filtration and the obtained filtrate consisted of a clear violet solution. Finally, the violet filtrate solution was left for slow evaporation at room temperature in a closed flask with a tiny hole. Large violet single crystals 6 were isolated after one month suitable for X-ray diffraction analysis (40% yield). Crystallization can be fastened to four days if a larger hole is used to evaporate the solvent from the covered mixture flask. FT-IR  $\nu$  (cm<sup>−1</sup>): 3092.1, 1596.3, 1492.9, 1402.2, 1211.9, 1087.7, 973.4, 927.5, 693.3. UV-visible:  $\lambda$ max: 307 nm, with shoulders at 277, 287, 302 nm.

## 4. Conclusions

*Trans*-CuCl<sub>2</sub>L<sub>2</sub> complex is square planar with 1,2,4-triazole containing Schiff base as the ligand L. The ligand L (E)-(4-chlorophenyl)-N-(3-phenyl-4H-1,2,4-triazol-4-yl)methanimine was prepared in situ from the reaction of copper chloride with 4-(4-chlorobenzylideneamino)-

5-phenyl-2H-1,2,4-triazole-3(4H)-thione. The synthesized compounds were characterized by applying various spectroscopic techniques. Intermolecular H-bonds and  $\pi$ - $\pi$  interactions govern the supramolecular structure of the copper complex. The structure is further investigated by computational DFT studies. A thione-thiol tautomerism for the triazole compound was also investigated. The Schiff base 1,2,4-triazole copper chloride complex is expected to have high anticancer activity.

**Supplementary Materials:** The following are available online at <https://www.mdpi.com/article/10.3390/inorganics11010018/s1>, Table S1: Crystal data of copper(II) complex (6) trans-CuCl<sub>2</sub>L<sub>2</sub> (CCDC No. 2217976); Table S2: Computed Energies and Cartesian Coordinates for copper(II) complex (6) trans-CuCl<sub>2</sub>L<sub>2</sub>; Table S3: Calculations of selected bond lengths for the copper(II) complex (6) using higher basis set; Table S4: Reaction Energies and Bond Dissociation Energies for Tautomer (3) and (3A); Figure S1: UV-visible spectrum of the copper complex (6); Figure S2: The correlation between experimental and computed values for the selected bond lengths present in the copper(II) complex (6) using pure and hybrid functionals with 6-31G(d)/LanL2DZ mixed basis set; Figure S3: A comparative correlation to evaluate the performance of various basis sets using CAM-B3LYP method for experimental and calculated bond lengths, for the selected bond lengths present in the copper(II) complex (6).

**Author Contributions:** H.H.H. and N.S.S. conceptualized, designed, supervised and acquired the funding for the project; M.W. performed the synthesis under the supervision of H.H.H. and M.M.A.-G.; Z.A.G. carried out X-ray analysis; M.H.S.A.H. and N.S.S. performed the computational investigation. All authors analyzed the results and were involved in writing the manuscript. Both H.H.H. and N.S.S. edited to generate the final version of the manuscript, agreed by all the authors. All authors have read and agreed to the published version of the manuscript.

**Funding:** This work was supported by the Deanship of Scientific Research, Vice Presidency for Graduate Studies and Scientific Research, King Faisal University, Saudi Arabia (Grant No. 2106).

**Institutional Review Board Statement:** Not applicable.

**Informed Consent Statement:** Not applicable.

**Data Availability Statement:** All data are available in the main text or the electronic supplementary information (ESI). See DOI: CCDC No. 2217976 contains the supplementary crystallographic data for this paper. These data can be obtained free of charge at [www.ccdc.cam.ac.uk](http://www.ccdc.cam.ac.uk) (accessed on 13 November 2022), or from the Cambridge Crystallographic Data Centre (CCDC), 12 Union Road, Cambridge CB2 1EZ, UK (fax: +44 1223 336033; e-mail: [deposit@ccdc.cam.ac.uk](mailto:deposit@ccdc.cam.ac.uk)).

**Acknowledgments:** This work was supported by the Deanship of Scientific Research, Vice Presidency for Graduate Studies and Scientific Research, King Faisal University, Saudi Arabia (Grant No. 2106). Both M.H.S.A.H. and N.S.S. thank the Universiti Brunei Darussalam for the research grant (UBD/RSCH/1.4/FICBF(b)/2022/049).

**Conflicts of Interest:** There are no conflict to declare.

**Sample Availability:** The samples of novel synthesized compounds are available from the authors.

## References

1. Omar, M.E.A.M.; Aboulwafa, M.O. Synthesis and in vitro antimicrobial and antifungal properties of some novel 1,3,4-thiadiazole and s-triazolo[3,4-b][1,3,4]thiadiazole derivatives. *J. Heterocycl. Chem.* **1986**, *23*, 1339–1341. [[CrossRef](#)]
2. Ding, Q.; Lei, X.; Jin, J.; Zhang, L.; Du, H.; Zhang, H. Synthesis and structure of novel 1,2,4-triazole derivatives containing the 2,4-dinitrophenylthio group. *Int. J. Chem. Res.* **2009**, *2*, 114–119. [[CrossRef](#)]
3. Heeres, J.; Backx, L.J.; Van Custen, J. Antimycotic azoles 7. Synthesis and antifungal properties of a series of novel triazol-3-ones. *J. Med. Chem.* **1984**, *27*, 894–900. [[CrossRef](#)]
4. Al-Masoudi, I.A.; Al-Soud, Y.A.; Al-Salihi, N.J.; Al-Masoudi, N.A. 1,2,4-Triazoles: Synthetic approaches and pharmacological importance. (Review). *Chem. Heterocycl. Compd.* **2006**, *42*, 1377–1403. [[CrossRef](#)]
5. Raman, N.; Joseph, J.; Kumar, S.M.; Sujatha, S.; Sahayaraj, K. Insecticidal activity of the schiff-base derived from anthranilic acid and acetoacetanilide and its copper complex on *Spodoptera litura* (Fab.). *J. Biopestic.* **2008**, *1*, 206–209.

6. Buvaylo, E.A.; Nesterova, O.V.; Goresnik, E.A.; Vyshniakova, H.V.; Petrusenko, S.R.; Nesterov, D.S. Supramolecular Diversity, Theoretical Investigation and Antibacterial Activity of Cu, Co and Cd Complexes Based on the Tridentate N,N,O-Schiff Base Ligand Formed In Situ. *Molecules* **2022**, *27*, 8233. [[CrossRef](#)]
7. Olar, R.; Badea, M.; Chifiriuc, M.C. Metal Complexes-A Promising Approach to Target Biofilm Associated Infections. *Molecules* **2022**, *27*, 758. [[CrossRef](#)]
8. Naito, Y.; Akahoshi, F.; Takeda, S.; Okada, T.; Kajii, M.; Nishimura, H.; Sugiura, M.; Fukaya, C.; Kagitani, Y. Synthesis and pharmacological activity of triazole derivatives inhibiting eosinophilia. *J. Med. Chem.* **1996**, *39*, 3019–3029. [[CrossRef](#)]
9. Kamboj, V.K.; Verma, P.K.; Dhanda, A.; Ranjan, S. 1,2,4-triazole derivatives as potential scaffold for anticonvulsant activity. *Cent. Nerv. Syst. Agents Med. Chem.* **2015**, *15*, 17–22. [[CrossRef](#)]
10. Chiu, S.-H.L.; Huskey, S.-E.W. Species differences in N-glucuronidation: 1996 ASPET N-glucuronidation of xenobiotics symposium. *Drug Metab. Dispos.* **1998**, *26*, 838–847.
11. Gomathinayagam, M.; Abdul Jaleel, C.; Lakshmanan, G.M.A.; Panneerselvam, R. Changes in carbohydrate metabolism by triazole growth regulators in cassava (*Manihot esculenta* Crantz); effects on tuber production and quality. *C. R. Biol.* **2007**, *330*, 644–655. [[CrossRef](#)] [[PubMed](#)]
12. Matela, G. Schiff Bases and Complexes: A Review on Anti-Cancer Activity. *Anticancer Agents Med. Chem.* **2020**, *20*, 1908–1917. [[CrossRef](#)]
13. Wu, J.; Liu, X.; Cheng, X.; Cao, Y.; Wang, D.; Li, Z.; Xu, W.; Pannecouque, C.; Witvrouw, M.; De Clercq, E. Synthesis of Novel Derivatives of 4-Amino-3-(2-Furyl)-5-Mercapto-1,2,4-Triazole as Potential HIV-1 NNRTIs. *Molecules* **2007**, *12*, 2003–2016. [[CrossRef](#)] [[PubMed](#)]
14. Mullicans, M.D.; Wilson, M.W.; Connor, D.T.; Kostlan, C.R.; Schrier, D.J.; Dyer, R.D. Design of 5-(3,5-di-tert-butyl-4-hydroxyphenyl)-1,3,4-thiadiazoles, -1,3,4-oxadiazoles, and -1,2,4-triazoles as orally active, nonulcerogenic antiinflammatory agents. *J. Med. Chem.* **1993**, *36*, 1090–1099. [[CrossRef](#)] [[PubMed](#)]
15. Slivka, M.V.; Korol, N.I.; Fizer, M.M. Fused bicyclic 1,2,4-triazoles with one extra sulfur atom: Synthesis, properties, and biological activity. *J. Heterocycl. Chem.* **2020**, *57*, 3236–3254. [[CrossRef](#)]
16. Kaur, R.; Ranjan, D.A.; Kumar, B.; Kumar, V. Recent Developments on 1,2,4-Triazole Nucleus in Anticancer Compounds: A Review. *Anti-Cancer Agents Med. Chem.* **2016**, *16*, 465–489. [[CrossRef](#)]
17. Wright, G.D. Resisting resistance: New chemical strategies for battling superbugs. *Chem. Biol.* **2000**, *7*, R127–R132. [[CrossRef](#)]
18. Travis, J.; Potempa, J. *Biochimica et Biophysica Acta (BBA) - Protein Structure and Molecular Enzymology*. *Biochim. Biophys. Acta* **2000**, *14*, 35–50. [[CrossRef](#)]
19. Smith, H.J.; Simons, C. *Proteinase and Peptidase Inhibition: Recent Potential Targets for Drug Development*; Taylor and Francis: London, UK, 2001.
20. Rice, S.A.; Givskov, M.; Steinberg, P.; Kjelleberg, S.J. Bacterial Signals and Antagonists: The Interaction Between Bacteria and Higher Organisms. *Mol. Microbiol. Biotechnol.* **1999**, *1*, 23–31.
21. Scozzafava, A.; Supuran, C.T. Carbonic Anhydrase and Matrix Metalloproteinase Inhibitors: Sulfonated Amino Acid Hydroxamates with MMP Inhibitory Properties Act as Efficient Inhibitors of CA Isozymes I, II, and IV, and N-Hydroxysulfonamides Inhibit Both These Zinc Enzymes. *J. Med. Chem.* **2000**, *43*, 3677–3687. [[CrossRef](#)]
22. Drabent, K.; Bialoska, A.; Ciunik, Z. New porous crystals of Cu(I) complexes with Schiff-base-containing triazole ligands. *Inorg. Chem. Commun.* **2004**, *7*, 224–227. [[CrossRef](#)]
23. Bazhin, D.N.; Kudryakova, Y.S.; Slepukhin, P.A.; Burgart, Y.V.; Malysheva, N.N.; Kozitsina, A.N.; Ivanova, A.V.; Bogomyakov, A.S.; Saloutin, V.I. Dinuclear copper(II) complex with novel N,N',N'',O-tetradentate Schiff base ligand containing trifluoromethylpyrazole and hydrazone moieties. *Mendeleev Commun.* **2018**, *28*, 202–204. [[CrossRef](#)]
24. Naik, A.D.; Annigeri, S.M.; Gangadharmath, U.B.; Ravankar, V.K.; Mahale, V.B.; Reddy, V.K. Anchoring mercapto-triazoles on dicarbonyl backbone to assemble novel binucleating, acyclic SNONS compartmental ligands. *Indian J. Chem.* **2002**, *41A*, 2046–2053.
25. Mazzoni, R.; Roncaglia, F.; Rigamonti, L. When the Metal Makes the Difference: Template Syntheses of Tridentate and Tetradentate Salen-Type Schiff Base Ligands and Related Complexes. *Crystals* **2021**, *11*, 483. [[CrossRef](#)]
26. Chohan, Z.H.; Pervez, H.; Khan, K.M.; Supuran, C.T. Organometallic-based antibacterial and antifungal compounds: Transition metal complexes of 1,1'-diacetylferrocene-derived thiocarbohydrazone, carbohydrazone, thiosemicarbazone and semicarbazone. *J. Enz. Inhib. Med. Chem.* **2005**, *20*, 81–88. [[CrossRef](#)]
27. Palmer, M.H.; Christen, D. An ab initio study of the structure, tautomerism and molecular properties of the C- and N-amino-1,2,4-triazoles. *J. Mol. Struct.* **2004**, *705*, 177–187. [[CrossRef](#)]
28. Singh, K.; Barwa, M.S.; Tyagi, P. Synthesis, characterization and biological studies of Co(II), Ni(II), Cu(II) and Zn(II) complexes with bidentate Schiff bases derived by heterocyclic ketone. *Eur. J. Med. Chem.* **2006**, *41*, 147–153. [[CrossRef](#)]
29. Chohan, Z.H.; Scozzafava, A.; Supuran, C.T. Unsymmetrical 1,1'-disubstituted Ferrocenes: Synthesis of Co(ii), Cu(ii), Ni(ii) and Zn(ii) Chelates of Ferrocenyl -1-thiadiazolo-1'-tetrazole, -1-thiadiazolo-1'-triazole and -1-tetrazolo-1'-triazole with Antimicrobial Properties. *J. Enz. Inhib. Med. Chem.* **2002**, *17*, 261–266. [[CrossRef](#)]
30. Klingele, M.H.; Brooker, S. The coordination chemistry of 4-substituted 3,5-di(2-pyridyl)-4H-1,2,4-triazoles and related ligands. *Coord. Chem. Rev.* **2003**, *241*, 119–132. [[CrossRef](#)]

31. Arion, V.B.; Reisner, E.; Fremuth, M.; Jokupec, M.A.; Keppler, B.K.; Kukushkin, V.Y.; Pombeiro, A.J.L. Synthesis, X-ray Diffraction Structures, Spectroscopic Properties, and in vitro Antitumor Activity of Isomeric (1H-1,2,4-Triazole)Ru(III) Complexes. *Inorg. Chem.* **2003**, *42*, 6024–6031. [[CrossRef](#)]
32. El-Masry, A.H.; Fahmy, H.H.; Abdelwahed, S.H.A. Synthesis and antimicrobial activity of some new benzimidazole derivatives. *Molecules* **2000**, *5*, 1429–1438. [[CrossRef](#)]
33. Pandeya, S.N.; Sriram, D.; Nath, G.; De Clereq, E. Synthesis and antimicrobial activity of Schiff and Mannich bases of isatin and its derivatives with pyrimidine. *IL Farmaco* **1999**, *54*, 624–628. [[CrossRef](#)] [[PubMed](#)]
34. Singh, W.M.; Dash, B.C. Synthesis of some new Schiff bases containing thiazole and oxazole nuclei and their fungicidal activity. *Pesticides* **1988**, *22*, 33–37.
35. Desai, S.B.; Desai, P.B.; Desai, K.R. Synthesis of some Schiff bases, thiazolidinones and azetidinones derived from 2, 6-diaminobenzo [1, 2-d: 4, 5-d'] bisthiazole and their anticancer activities. *Heterocycl. Commun.* **2001**, *7*, 83–90. [[CrossRef](#)]
36. Pathak, P.; Jolly, V.S.; Sharma, K.P. Synthesis and Biological Activities of Some New Substituted Arylazo Schiff Bases. *Orient. J. Chem.* **2000**, *16*, 161–162.
37. Samadhiya, S.; Halve, A. Synthetic Utility of Schiff Bases as Potential Herbicidal Agents. *Orient. J. Chem.* **2001**, *17*, 119–122.
38. Karegoudar, P.; Karthikeyan, M.S.; Prasad, D.J.; Mahalinga, M.; Holla, B.S.; Kumari, N.S. Synthesis of some novel 2,4-disubstituted thiazoles as possible antimicrobial agents. *Eur. J. Med. Chem.* **2008**, *43*, 261–267. [[CrossRef](#)]
39. Jubie, S.; Sikdar, P.; Antony, S.; Kalirajan, R.; Gowramma, B.; Gomathy, S.; Elango, K. Synthesis and biological evaluation of some Schiff bases of [4-(amino)-5-phenyl-4H-1,2,4-Triazole-3-Thiol]. *Pak. J. Pharm. Sci.* **2011**, *24*, 109–112.
40. El Ashry, E.S.H.; Kassem, A.A.; Abdel-Hamid, H.; Louis, F.F.; Khattab, S.A.N.; Aouad, M.R. Synthesis of 4-amino-5-(3-chlorobenzo[b]thien-2-yl)-3-mercapto-1,2,4-triazolo[3,4-b][1,3,4]thiadiazoles and triazolo[3,4,b][1,3,4]thiadiazines under classical and microwave conditions. *Arkivoc* **2006**, (14), 119–132.
41. Mange, Y.J.; Isloor, A.M.; Malladi, S.; Isloor, S. Synthesis and antimicrobial activities of some novel 1,2,4-triazole derivatives. *Arab J. Chem.* **2013**, *6*, 177–181.
42. Zhou, S.; Zhang, L.; Jin, J.; Zhang, A.; Lei, X.; Lin, J.; He, J.; Zhang, H. Synthesis and Biological Activities of Some Novel Triazolothiadiazines and Schiff Bases Derived from 1,2,4-Triazole. *Phosphorus Sulfur Silicon* **2007**, *182*, 419–432. [[CrossRef](#)]
43. Liu, X.Y.; Xu, W.F.; Wu, J.D. Synthesis of 4-Amino-5-furyl-2-yl-4H-1, 2, 4-triazole-3-thiol derivatives as a Novel Class of Endothelin (ET) Receptor Antagonists. *Chin. Chem. Lett.* **2003**, *14*, 790–793.
44. Kabbani, A.T.; Zaworotko, M.J.; Abourahma, H.; Bailly Walsh, R.D.; Hammud, H.H. Supramolecular Structure of Tetrakis- $\mu$ -[4-Chloro-3-nitrobenzoato]bis(methanol)dicopper(II)]. *J. Chem. Crystallogr.* **2004**, *34*, 749–756. [[CrossRef](#)]
45. Zaworotko, M.J.; Hammud, H.H.; Kravtsov, V.C. The co-crystal of iron(II) complex hydrate with hydroxybenzoic acid: [Fe(Phen)3]Cl(p-hydroxybenzoate).2(p-hydroxybenzoic acid).7H<sub>2</sub>O. *J. Chem. Crystallogr.* **2007**, *27*, 219–231. [[CrossRef](#)]
46. Hammud, H.H.; Holman, K.T.; Masoud, M.S.; El-Faham, A.; Beidas, H. 1-Hydroxybenzotriazole (HOBt) acidity, formation constant with different metals and thermodynamic parameters. Synthesis and characterization of some HOBt metal complexes. Crystal structures of two polymers: [Cu<sub>2</sub>(H<sub>2</sub>O)<sub>5</sub>(OBt)<sub>2</sub>( $\mu$ -OBt)<sub>2</sub>].2H<sub>2</sub>O.EtOH (1A) and [Cu( $\mu$ -OBt)(HOBt)(OBt)(EtOH)] (1B). *Inorg. Chim. Acta* **2009**, *362*, 3526–3540.
47. Hammud, H.H.; Kortz, U.; Bhattacharya, S.; Demirdjian, S.; Hariri, E.; Isber, S.; Sang Choi, E.; Mirtamizdoust, B.; Mroueh, M.; Daher, C.F. Structure, DFT studies, Magnetism and Biological activity of Bis[( $\mu$ 2-azido)-chloro-(1,10-phenanthroline)-copper(II)] complex. *Inorg. Chim. Acta* **2020**, *506*, 119533. [[CrossRef](#)]
48. Hammud, H.H.; Zaworotko, M.J.; McManus, G.J.; Tabesh, R.N.; Islam, H.; Ibrahim, M.; Ayub, K.; Ludwig, R. The co-crystal of copper(II) phenanthroline chloride complex hydrate with p-aminobenzoic acid: Structure, cytotoxicity, thermal analysis and DFT calculation. *Chem. Mon.* **2021**, *152*, 323–336. [[CrossRef](#)]
49. Zaworotko, M.; Hammud, H.; Abbas, I.; Kravtsov, V.; Masoud, M. Ampicillin acidity and formation constants with some metals and their thermodynamic parameters in different media. Crystal structures of two polymorphs isolated from the reaction of ampicillin with copper(II). *J. Coord. Chem.* **2006**, *59*, 65–84. [[CrossRef](#)]
50. Hammud, H.H.; Nemer, G.; Sawma, W.; Touma, J.; Barnabe, P.; Bou-Mouglabey, Y.; Ghannoum, A.; El-Hajjar, J.; Usta, J. Copper-adenine complex, a compound, with multi-biochemical targets and potential anti-cancer effect. *Chem. Biol. Interact.* **2008**, *173*, 84–96. [[CrossRef](#)]
51. Mroueh, M.; Daher, C.; Hariri, E.; Demirdjian, S.; Isber, S.; Choi, E.S.; Mirtamizdoust, B.; Hammud, H.H. Magnetic property, DFT calculation, and biological activity of bis[( $\mu$ 2-chloro)chloro(1,10-phenanthroline)copper(II)] complex. *Chem. Biol. Interact.* **2015**, *231*, 53–60. [[CrossRef](#)]
52. Hammud, H.H.; Holman, K.T.; Al-Noaimi, M.; Sheikh, N.S.; Ghannoum, A.M.; Bouhadir, K.H.; Masoud, M.S.; Karnati, R.K. Structures of selected transition metal complexes with 9-(2-hydroxyethyl)adenine: Potentiometric complexation and DFT Studies. *J. Mol. Struct.* **2020**, *1205*, 127548. [[CrossRef](#)]
53. Parr, R.G.; Yang, W. *Density-Functional Theory of Atoms and Molecules*; Oxford University Press: Oxford, UK, 1989.
54. Frisch, M.J.; Trucks, G.W.; Schlegel, H.B.; Scuseria, G.E.; Robb, M.A.; Cheeseman, J.R.; Scalmani, G.; Barone, V.; Mennucci, B.; Petersson, G.A.; et al. *Gaussian 09*; Revision E.01; Gaussian, Inc.: Wallingford, CT, USA, 2013.
55. Dennington, R.; Keith, T.; Millam, J. *GaussView, Version 5*; Semichem Inc.: Shawnee Mission, KS, USA, 2009.
56. Becke, A.D. Density-functional thermochemistry. III. The role of exact exchange. *J. Chem. Phys.* **1993**, *98*, 5648. [[CrossRef](#)]
57. Becke, A.D. A new mixing of Hartree-Fock and local density-functional theories. *J. Chem. Phys.* **1993**, *98*, 1372. [[CrossRef](#)]

58. Lee, C.; Yang, W.; Parr, R.G. Development of the Colle-Salvetti correlation-energy formula into a functional of the electron density. *Phys. Rev. B* **1988**, *37*, 785. [[CrossRef](#)] [[PubMed](#)]
59. Yanai, T.; Tew, D.P.; Handy, N.C. A new hybrid exchange-correlation functional using the Coulomb-attenuating method (CAM-B3LYP). *Chem. Phys. Lett.* **2004**, *393*, 51. [[CrossRef](#)]
60. Becke, A.D. Density-functional exchange-energy approximation with correct asymptotic behavior. *Phys. Rev. A* **1988**, *38*, 3098. [[CrossRef](#)]
61. Adamo, C.; Barone, V.J. Exchange functionals with improved long-range behavior and adiabatic connection methods without adjustable parameters: The *m*PW and *m*PW1PW models. *Chem. Phys.* **1998**, *108*, 664. [[CrossRef](#)]
62. Chai, J.-D.; Head-Gordon, M. Long-range corrected hybrid density functionals with damped atom-atom dispersion corrections. *Phys. Chem. Chem. Phys.* **2008**, *10*, 6615. [[CrossRef](#)]
63. Perdew, J.P.; Burke, K.; Ernzerhof, M. Generalized gradient approximation made simple. *Phys. Rev. Lett.* **1996**, *77*, 3865. [[CrossRef](#)]
64. Hay, P.J.; Wadt, W.R. *Ab initio* effective core potentials for molecular calculations. Potentials for the transition metal atoms Sc to Hg. *J. Chem. Phys.* **1985**, *82*, 270–283. [[CrossRef](#)]
65. Wadt, W.R.; Hay, P.J. *Ab initio* effective core potentials for molecular calculations. Potentials for main group elements Na to Bi. *J. Chem. Phys.* **1985**, *82*, 284–298. [[CrossRef](#)]
66. Hay, P.J.; Wadt, W.R. *Ab initio* effective core potentials for molecular calculations. Potentials for K to Au including the outermost core orbitals. *J. Chem. Phys.* **1985**, *82*, 299–310. [[CrossRef](#)]
67. How, F.N.-F.; Crouse, K.A.; Tahir, M.I.M.; Tarafder, M.; Cowley, A.R. Synthesis, characterization and biological studies of S-benzyl- $\beta$ -N-(benzoyl) dithiocarbamate and its metal complexes. *Polyhedron* **2008**, *27*, 3325–3329. [[CrossRef](#)]
68. Li, X.; Li, X.-Q.; Liu, H.-M.; Zhou, X.-Z.; Shao, Z.-H. Synthesis and evaluation of antitumor activities of novel chiral 1,2,4-triazole Schiff bases bearing  $\gamma$ -butenolide moiety. *Org. Med. Chem. Lett.* **2012**, *2*, 26. [[CrossRef](#)] [[PubMed](#)]
69. Li, Z.; Gu, Z.; Yin, K.; Zhang, R.; Deng, Q.; Xiang, J. Synthesis of substituted-phenyl-1,2,4-triazol-3-thione analogues with modified D-glucopyranosyl residues and their antiproliferative activities. *Eur. J. Med. Chem.* **2009**, *44*, 4716–4720. [[CrossRef](#)]
70. Wang, B.-L.; Zhang, L.-Y.; Liu, X.-H.; Ma, Y.; Zhang, Y.; Li, Z.-M.; Zhang, X. Synthesis, biological activities and SAR studies of new 3-substitutedphenyl-4-substitutedbenzylideneamino-1,2,4-triazole Mannich bases and bis-Mannich bases as ketol-acid reductoisomerase inhibitors. *Bioorganic Med. Chem. Lett.* **2017**, *27*, 5457–5462. [[CrossRef](#)]

**Disclaimer/Publisher's Note:** The statements, opinions and data contained in all publications are solely those of the individual author(s) and contributor(s) and not of MDPI and/or the editor(s). MDPI and/or the editor(s) disclaim responsibility for any injury to people or property resulting from any ideas, methods, instructions or products referred to in the content.